Matrix continued-fraction solution for saturation effects in spin-1/2 radio-frequency spectroscopy

M. Allegrini*
Laboratorio di Fisica Atomica e Molecolare del Consiglio Nazionale delle Ricerche, Via del Giardino 3, 56100 Pisa, Italy

E. Arimondo*
Istituto di Fisica dell'Università, Piazza Torricelli 2, 56100 Pisa, Italy

A. Bambini
Laboratorio di Elettronica Quantistica del Consiglio Nazionale delle Ricerche, Via Panciatichi 56/30, 50127 Firenze, Italy

(Received 13 September 1976)

We present a semiclassical solution for a Zeeman-split, optically pumped, spin-1/2 system interacting with a strong radio-frequency field. The method of solution presented here is based upon a matrix continued-fraction expansion, and can explain any resonance phenomena which occur for arbitrary geometrical configurations of the pumping beam or the rf field polarization axis. Theoretical predictions of line shapes for some cases are reported and discussed. The solution can also explain some deviations of the observed Bloch-Siegert shift at high rf power from the behavior predicted by a previous semiclassical theory, which can account for simple geometrical configurations only.

I. INTRODUCTION

Much work has been devoted to investigating the phenomena occurring in a spin-$\frac{1}{2}$ system (a two-level system), whose levels are split by a static magnetic field, and connected through a magnetic-dipole interaction with a radio-frequency magnetic field. Experiments have been performed on the ground state of several atomic species, in optically pumped atomic vapors. In these experiments, the static field is usually perpendicular to the rf polarization axis, while the pumping light beam is directed along the static field (longitudinal pumping) or perpendicular to it (transverse pumping). Other experiments have been performed with a configuration where the static and the rf polarization axis are parallel (parametric resonance).

The polarization of the pump beam is chosen in such a way that the beam acts selectively on either of the two levels involved in the transition. Then in the longitudinal pumping, the pumping cycle creates a difference in the populations, i.e., in the diagonal elements of the atomic density matrix. In the transverse pumping, the light beam creates coherences, i.e., the off-diagonal elements are nonzero.

Several semiclassical or fully quantum-mechanical methods have been developed to interpret the experimental results. Owing to the large number of photons in the rf field, even at small intensities, the semiclassical theory seems to predict correctly all phenomena occurring in the transitions. Moreover, it may treat phenomenologically any incoherent relaxation mechanism, as well as the pumping mechanism. The semiclassical theory has been developed by several authors to describe phenomena occurring in different configurations of the magnetic fields or pumping beam. Favre and Geneux[1] found the steady-state solution for the density matrix elements in the parametric resonance, through an expansion in a series of Bessel functions. For an oscillating field perpendicular to the static one, a continued fraction solution has been derived, in the case of longitudinal pumping by Stenholm[2,3] and in the case of transverse pumping by Stenholm and Aminoff[4] and Tsukada and Ogawa.[5]

A proper description of actual experiments has to include deviations from these geometries for the rf and static fields and the pump beam. Several authors have described the phenomena arising with the misalignment of the rf field from the direction along the static field or perpendicularly to it, with the presence of an uncompensated stray field and with the misalignment of the light beam with competition of longitudinal and transverse pumping.[6-9] Different treatments have been developed to describe the influence of a small misalignment present in the experiments. The line shape of the resonances for an experiment of longitudinal pumping with an arbitrary angle between the oscillating and static fields has been investigated by Yabuzaki *et al.*[10] The nu-

merical solution of a very large set of simultaneous linear equations, derived from the time evolution equations for the density matrix, has been applied to interpret their experimental results.

It has been shown by one of us[11] that the density matrix elements of a two-level system, which interacts with a high-intensity field, made up of several modes, may be found by means of a continued fraction expansion, whose terms are matrices. The solution applies in the semiclassical laser theory when the atoms are fixed in the space, and the electromagnetic modes are equally spaced in frequency. There is a close resemblance between that situation and rf spectroscopy, since in the latter case the vapor atoms are confined in a small cell, whose dimensions are negligible in comparison with the wavelength of the electromagnetic field. Therefore, a matrix continued fraction expansion for the elements of the density matrix is expected to solve the rf spectroscopy problem with any configuration of magnetic fields or the pumping beam.

The purpose of this paper is to show that such solution exists, and to use it in discussing several cases of interest. For numerical calculations the continued fraction is very useful, since the convergence of the solution can easily be tested. Moreover, in truncating at some order of the continued fraction expansion the contributions of that order are neglected altogether.

In Sec. II, the basic equations of motion are derived, and the Fourier transformed equation of motion for the out-of-phase polarization is obtained. In Sec. III, the matrix continued fraction solution is presented, and a comparison is made with the previous results obtained by Stenholm.[2-4] These results are recovered as a limiting case of our treatment. In Sec. IV, some numerical applications of the general solution are presented. The conclusions are presented in Sec. V.

II. DENSITY-MATRIX EQUATION OF MOTION

Let us consider an experiment on an ensemble of spin-$\frac{1}{2}$ atoms in the ground state. These two levels are split by a static magnetic field H_0, and a pumping light beam removes them from their thermal equilibrium. An oscillating magnetic field $H_1 \cos\omega t$ induces transitions between them. The directions of these fields and of the light beam are drawn in Fig. 1. The z axis is directed along the static magnetic field. In order to allow for any possible planar misalignment, the pumping light beam and the rf field have arbitrary directions in the x-z plane. Two special cases are included in the general treatment; they are the

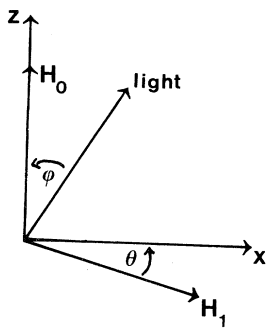

FIG. 1. Orientations of the H_0 static field, the H_1 radio-frequency field and the pumping beam.

longitudinal and the transverse pumping. The former is achieved with the light beam perpendicular to the static field, while the latter is generated with the light beam perpendicular to the static field. In most experiments, both these resonances are caused by a rf field perpendicular to the static field. In our analysis the rf field-polarization axis is kept arbitrary, in order to allow us to discuss any misalignment effect.

We choose the z axis as the quantization axis for the quantum treatment of the atomic system. This choice is made on physical grounds. In fact, in this quantization scheme, we can allow for different longitudinal and transverse decay rates of the density-matrix components. In order to show this, let us briefly summarize the process of pumping.

Let $|a\rangle$ and $|b\rangle$ be, respectively, the upper and the lower levels of the ground state, in the scheme where the quantization axis is directed along the pumping light beam. The pumping process is an incoherent process, so that its net effect will be that of generating different populations in the two levels $|a\rangle$ and $|b\rangle$. Let us call Δ the population difference as created by the pumping process

$$\Delta = \rho_{aa}^{(0)} - \rho_{bb}^{(0)} . \tag{1}$$

If the two levels are removed from their steady state, they will regain it with the equations of motion

$$\dot{\rho}_{aa} - \dot{\rho}_{bb} = -\gamma(\rho_{aa} - \rho_{bb} - \Delta) , \tag{2a}$$

$$\dot{\rho}_{ab} + \dot{\rho}_{ba} = -\gamma(\rho_{ab} + \rho_{ba}) , \tag{2b}$$

$$\dot{\rho}_{ab} - \dot{\rho}_{ba} = -\gamma(\rho_{ab} - \rho_{ba}) . \tag{2c}$$

The pump rates γ at which the diagonal and the off-diagonal elements reach the steady state values are the same. Let us now rotate the axis of quantization by an angle φ, making the quantization axis to coincide with the z axis (the axis of the static magnetic field). In this scheme, let $|-\rangle$ and $|+\rangle$ be, respectively, the upper and the lower levels.

Equations (2) in this scheme now read

$$\dot{\rho}_{--} - \dot{\rho}_{++} = -\gamma(\rho_{--} - \rho_{++}) + \lambda\cos\varphi\,, \tag{3a}$$

$$\dot{\rho}_{-+} + \dot{\rho}_{+-} = -\gamma(\rho_{-+} + \rho_{+-}) + \lambda\sin\varphi\,, \tag{3b}$$

$$\dot{\rho}_{-+} - \dot{\rho}_{+-} = -\gamma(\rho_{-+} - \rho_{+-})\,. \tag{3c}$$

where $\lambda = \gamma\Delta$. The $|-\rangle$ and $|+\rangle$ states are the energy levels of the atomic system in the static magnetic field. They relax, in the absence of an external pumping mechanism, towards a state of equal populations, with a rate γ_1', the longitudinal decay rate. Their coherence (i.e., the off-diagonal elements) relaxes to zero with a rate γ_2' which may be greater than γ_1'. The relaxation and the pumping process are incoherent. Then we are allowed to add up the decay rates, and, defining

$$\gamma_1 = \gamma_1' + \gamma, \quad \gamma_2 = \gamma_2' + \gamma\,,$$

the equations of motion for the density-matrix elements (including contributions from the static-field Hamiltonian) are readily written

$$\dot{\rho}_{--} - \dot{\rho}_{++} = \lambda\cos\varphi - \gamma_1(\rho_{--} - \rho_{++})\,, \tag{4a}$$

$$\dot{\rho}_{-+} + \dot{\rho}_{+-} = \lambda\sin\varphi - \gamma_2(\rho_{-+} + \rho_{+-}) - i\omega_0(\rho_{-+} - \rho_{+-})\,, \tag{4b}$$

$$\dot{\rho}_{-+} - \dot{\rho}_{+-} = -\gamma_2(\rho_{-+} - \rho_{+-}) - i\omega_0(\rho_{-+} + \rho_{+-})\,, \tag{4c}$$

where ω_0 is the frequency separation of the two levels, i.e., $\omega_0 = \gamma_G H_0$, and γ_G is the gyromagnetic ratio. To these equations we must add the interaction term with the rf field. Let θ denote the misalignment angle of the rf field, i.e., the angle between the direction of the rf field and the x axis as indicated in Fig. 1. Then the complete set of equations to be solved is given by

$$i(\dot{\rho}_{--} - \dot{\rho}_{++}) = i\lambda\cos\varphi - i\gamma_1(\rho_{--} - \rho_{++}) + \omega_1\cos\theta\cos\omega t(\rho_{-+} - \rho_{+-})\,, \tag{5a}$$

$$i(\dot{\rho}_{-+} + \dot{\rho}_{+-}) = i\lambda\sin\varphi - i\gamma_2(\rho_{-+} + \rho_{+-}) + (\omega_0 + \omega_1\sin\theta\cos\omega t)(\rho_{-+} - \rho_{+-})\,, \tag{5b}$$

$$i(\dot{\rho}_{-+} - \dot{\rho}_{+-}) = -i\gamma_2(\rho_{-+} - \rho_{+-}) + (\omega_0 + \omega_1\sin\theta\cos\omega t)(\rho_{-+} + \rho_{+-}) + \omega_1\cos\theta\cos\omega t(\rho_{--} - \rho_{++})\,, \tag{5c}$$

where $\omega_1 = \gamma_G H_1$. In order to find the solution to systems (5), the density-matrix components are expressed as a Fourier series

$$\rho_{--} - \rho_{++} = \sum_n d_n e^{in\omega t}, \tag{6a}$$

$$\rho_{-+} + \rho_{+-} = \sum_n c_n e^{in\omega t}, \tag{6b}$$

$$\rho_{-+} - \rho_{+-} = -i\sum_n s_n e^{in\omega t}. \tag{6c}$$

Owing to the particular choice of the Fourier expansions, each set of coefficients $\{d_n\}$, $\{c_n\}$, $\{s_n\}$ satisfies the relation

$$x_{-n} = x_n^*\,, \tag{7}$$

where x_n stands for d_n, c_n, s_n. In summations (6), even and odd components are included, since multiphoton transitions at all orders are allowed. The following set of equations is therefore derived:

$$(\gamma_1 + in\omega)d_n = \lambda\cos\varphi\,\delta_{n,0} - \tfrac{1}{2}\omega_1\cos\theta(s_{n+1} + s_{n-1})\,, \tag{8a}$$

$$(\gamma_2 + in\omega)c_n = \lambda\sin\varphi\,\delta_{0,n} - \omega_0 s_n - \tfrac{1}{2}\omega_1\sin\theta(s_{n+1} + s_{n-1})\,, \tag{8b}$$

$$(\gamma_2 + in\omega)s_n = \omega_0 c_n + \tfrac{1}{2}\omega_1\sin\theta(c_{n+1} + c_{n-1}) + \tfrac{1}{2}\omega_1\cos\theta(d_{n+1} + d_{n-1})\,. \tag{8c}$$

From this set of equations we obtain recurrence relations for the Fourier coefficients of any density-matrix component. The simplest recurrence relation is found for the s_n coefficients

$$P(n)s_{n-2} + Q(n)s_{n-1} + [1 + R(n)]s_n + S(n)s_{n+1} + T(n)s_{n+2} = X_0\delta_{0,n} + X_1\delta_{n,1} + X_{-1}\delta_{n,-1}\,, \tag{9}$$

with

$$P(n) = \tfrac{1}{4}\omega_1^2(\sin^2\theta F_{n-1} + \cos^2\theta E_{n-1})D_n\,, \tag{10a}$$

$$Q(n) = \tfrac{1}{2}\omega_0\omega_1\sin\theta(F_n + F_{n-1})D_n\,, \tag{10b}$$

$$S(n) = \tfrac{1}{2}\omega_0\omega_1\sin\theta(F_n + F_{n+1})D_n\,, \tag{10c}$$

$$T(n) = \tfrac{1}{4}\omega_1^2(\sin^2\theta F_{n+1} + \cos^2\theta E_{n+1})D_n\,, \tag{10d}$$

$$R(n) = P(n) + T(n)\,, \tag{10e}$$

$$X_0 = (1/\gamma_2)\lambda\sin\varphi\,\omega_0 D_0\,, \tag{10f}$$

$$X_{\pm 1} = \tfrac{1}{2}\lambda\omega_1(\gamma_2^{-1}\sin\varphi\sin\theta + \gamma_1^{-1}\cos\varphi\cos\theta)D_{\pm 1} \tag{10g}$$

and

$$D_n = \tfrac{1}{2}[\gamma_2 + i(n\omega - \omega_0)]^{-1} + \tfrac{1}{2}[\gamma_2 + i(n\omega + \omega_0)]^{-1}\,, \tag{11a}$$

$$E_n = (\gamma_1 + in\omega)^{-1}\,, \tag{11b}$$

$$F_n = (\gamma_2 + in\omega)^{-1}\,. \tag{11c}$$

Knowledge of the coefficients s_n allows one to evaluate, from (8a) and (8b), the coefficients d_n and c_n. Then the recurrence relation (9) is the basic equation to be solved, and in Sec. II we shall show how to solve it in terms of a continued fraction expansion, whose terms are matrices.

III. MATRIX CONTINUED FRACTION SOLUTION

In this section we describe the solution of the recurrence relation (9), with a matrix continued fraction expansion. The convergence and the uniqueness of the solution will not be treated here; a detailed discussion of these properties may be found in Ref. 11.

Let us consider the five central equations of (9), i.e., the equations with $n = 0, \pm 1, \pm 2$. This set forms a linear system with nine unknowns s_m, with $m = 0, \pm 1, \pm 2, \pm 3, \pm 4$:

$$P(-2)s_{-4} + Q(-2)s_{-3} + [1 + R(-2)]s_{-2} + S(-2)s_{-1} + T(-2)s_0 = 0, \quad (12a)$$

$$P(-1)s_{-3} + Q(-1)s_{-2} + [1 + R(-1)]s_{-1} + S(-1)s_0 + T(-1)s_1 = X_{-1}, \quad (12b)$$

$$P(0)s_{-2} + Q(0)s_{-1} + [1 + R(0)]s_0 + S(0)s_1 + T(0)s_2 = X_0, \quad (12c)$$

$$P(1)s_{-1} + Q(1)s_0 + [1 + R(1)]s_1 + S(1)s_2 + T(1)s_3 = X_1, \quad (12d)$$

$$P(2)s_0 + Q(2)s_1 + [1 + R(2)]s_2 + S(2)s_3 + T(2)s_4 = 0. \quad (12e)$$

Obviously, this system has not a unique solution. But if we handle with the other equations, the "wing" equations, of (9), we can express the four extra unknowns $s_{\pm 3}$, $s_{\pm 4}$ in terms of s_0, $s_{\pm 1}$, $s_{\pm 2}$, and substitute them in (12). Then the system (12) may be readily solved, and a unique solution is found for s_0, $s_{\pm 1}$, $s_{\pm 2}$. We proceed therefore to express the four unknowns $s_{\pm 3}$, $s_{\pm 4}$, in terms of the central unknowns s_0, $s_{\pm 1}$, $s_{\pm 2}$.

First of all, we note that the wing equations of (9), i.e., the equations with $n = \pm 3, \pm 4, \ldots$, link together the coefficients s_m with the same sign of m. Furthermore, s_0 does not appear in these equations. Therefore, the coefficients s_{+3} and s_{+4} are expressed as a function of s_{+1} and s_{+2}, and the coefficients s_{-3} and s_{-4} as a function of s_{-1} and s_{-2}. Owing to the linearity of the system (9), these relations must be also be linear, i.e.,

$$\begin{pmatrix} s_3 \\ s_4 \end{pmatrix} = Z_+ \begin{pmatrix} s_1 \\ s_2 \end{pmatrix} \quad (13)$$

and

$$\begin{pmatrix} s_{-3} \\ s_{-4} \end{pmatrix} = Z_- \begin{pmatrix} s_{-1} \\ s_{-2} \end{pmatrix}, \quad (14)$$

where Z_+ and Z_- are 2×2 matrices, which must be deduced from the wing equations of system (9). Actually, we need to evaluate Z_+ only (or, equivalently, Z_-), since the condition (7) implies

$$Z_- = (Z_+)^*. \quad (15)$$

In order to find the matrix Z_+, we write the wing equations of system (9), i.e., those with $n \geq 3$, in a matrix form

$$U_{p+1}N_{p+1} + V_p N_p + W_{p-1}N_{p-1} = 0 \quad (p = 2, 3, \ldots), \quad (16)$$

where N_p are vectors

$$N_p = \begin{pmatrix} s_{2p-1} \\ s_{2p} \end{pmatrix} \quad (17)$$

and U_p, V_p, W_p are 2×2 matrices

$$U_p = \begin{pmatrix} T(2p-3) & 0 \\ S(2p-2) & T(2p-2) \end{pmatrix}, \quad (18a)$$

$$V_p = \begin{pmatrix} 1 + R(2p-1) & S(2p-1) \\ Q(2p) & 1 + R(2p) \end{pmatrix}, \quad (18b)$$

$$W_p = \begin{pmatrix} P(2p+1) & Q(2p+1) \\ 0 & P(2p+2) \end{pmatrix}. \quad (18c)$$

We must search for the relation which links N_2 with N_1. If we put $N_3 = 0$, then the relation is easily found from (16):

$$N_2 = -(1/V_2)W_1N_1 = Z_+^{(3)}N_1 \quad (19)$$

where $1/V_2$ is the inverse of the matrix V_2. Similarly, if we put $N_4 = 0$, we obtain from (16), after some algebra,

$$N_2 = -\frac{1}{V_2 - U_3 \dfrac{1}{V_3} W_2} W_1 N_1 = Z_+^{(4)} N_1. \quad (20)$$

By putting successively $N_3 = 0$, $N_4 = 0$, $N_5 = 0, \ldots$, we obtain the succession of matrices $Z_+^{(3)}$, $Z_+^{(4)}$, $Z_+^{(5)}, \ldots$, which converges, as shown in Ref. 11, to the Z_+ matrix, which appears in (13). Therefore, the continued fraction expansion for the matrix Z_+ is given by

$$Z_+ = -\cfrac{1}{V_2 - U_3 \cfrac{1}{V_3 - U_4 \cfrac{1}{V_4 - \cdots} W_3} W_2} W_1. \quad (21)$$

As we have said at the beginning of this section, we shall not prove that the expansion (21) converges towards a definite limit. We only note that the convergence of (21) is a consequence of the fact that the five coefficients $P(n)$, $Q(n)$, $R(n)$, $S(n)$, and $T(n)$ tend to zero as $1/n^2$ when n tends to infinity. The matrix Z_+ may be computed as we shall describe in Sec. IV. When Z_+ is known, one can numerically solve the system (12), and find the coefficients s_0, $s_{\pm 1}$, $s_{\pm 2}$. In turn, know-

ledge of these coefficients, is sufficient to determine all other coefficients of interest in the Fourier expansions. For practical purposes, only a few Fourier coefficients are needed; i.e., those which enter the analytical expression of the monitored signal. For example, if we detect resonances in the static magnetization along a particular direction of the x-z plane, then the coefficients of interest are c_0 and d_0. When that direction coincides with the pumping light beam direction, as in most experiments it is made, the analytical expression of the monitored static magnetization is given by

$$\begin{aligned}\mathfrak{M} &= d_0\cos\varphi + c_0\sin\varphi \\ &= \lambda\left[\frac{\cos^2\varphi}{\gamma_1}+\frac{\sin^2\varphi}{\gamma_2}\right]-\frac{\omega_0 s_0\sin\varphi}{\gamma_2} \\ &\quad -\omega_1\,\mathrm{Re}s_1\left(\frac{\cos\varphi\cos\theta}{\gamma_1}+\frac{\sin\varphi\sin\theta}{\gamma_2}\right) . \end{aligned} \tag{22}$$

In order to gain some insight into the physical significance of the obtained solution, we shall discuss some special cases of the expansion (21). We observe that, when the static field is perpendicular to the rf field, the angle θ is zero, and the two coefficients $Q(n)$ and $S(n)$ vanish. Then the matrices U_p, V_p, and W_p are diagonal, and the matrix Z_+ has a diagonal form also:

$$Z_+ = -\begin{pmatrix} \mathfrak{A} & 0 \\ 0 & \mathfrak{B} \end{pmatrix} , \tag{23}$$

where

$$\mathfrak{A} = \cfrac{P(3)}{1+R(3)-\cfrac{T(3)P(5)}{1+R(5)-\cfrac{T(5)P(7)}{1+\cdots}}} \tag{24}$$

and

$$\mathfrak{B} = \cfrac{P(4)}{1+R(4)-\cfrac{T(4)P(6)}{1+R(6)-\cfrac{T(6)P(8)}{1+\cdots}}} . \tag{25}$$

We have, therefore, from (13) and (23):

$$s_3 = -\mathfrak{A}s_1 , \tag{26}$$

$$s_4 = -\mathfrak{B}s_2 . \tag{27}$$

With these relations and their complex conjugates we are now able to solve the system (12), which takes the form

$$\{-P(-2)\mathfrak{B}^* + [1+R(-2)]\}s_{-2} + T(-2)s_0 = 0 , \tag{28a}$$

$$\{-P(-1)\mathfrak{A}^* + [1+R(-1)]\}s_{-1} + T(-1)s_1 = X_{-1} , \tag{28b}$$

$$P(0)s_{-2} + [1+R(0)]s_0 + T(0)s_2 = X_0 , \tag{28c}$$

$$P(1)s_{-1} + \{[1+R(1)] - T(1)\mathfrak{A}\}s_1 = X_1 , \tag{28d}$$

$$P(2)s_0 + \{[1+R(2)] - T(2)\mathfrak{B}\}s_2 = 0 . \tag{28e}$$

It is seen that the system (28) splits into two mutually independent systems, one of them involving the unknowns s_{-2}, s_0, and s_{+2}, and the other the unknowns s_{-1} and s_{+1}. In this case, therefore, the longitudinal and the transverse pumpings act independently; the former creates a coherence $i(\rho_{+-}-\rho_{-+})$ which has only odd Fourier coefficients $(s_{-1}, s_{+1}, s_{\pm 3}, \ldots)$; the latter contributes only the even Fourier coefficients of $i(\rho_{+-}-\rho_{-+})$, i.e., $s_0, s_{-2}, s_{+2}, s_{\pm 4}, \ldots$. We give the solution to the longitudinal pumping as derived from (28). We have

$$s_1 = \frac{P(1)X_{-1} - [1+R^*(1) - T^*(1)\mathfrak{A}^*]X_1}{|P(1)|^2 - |1+R(1)-T(1)\mathfrak{A}|^2} . \tag{29}$$

This result coincides with that obtained by Stenholm,[2] although the continued fraction expansion which is given by (29) is a contracted form of the continued fraction expansion used by Stenholm. In order to show the equivalence of (29) and Eq. (22) in Stenholm's paper, we use the identity

$$1+R(1)-T(1)\mathfrak{A} = 1+P(1)+\cfrac{T(1)}{1+\cfrac{P(3)}{1+\cfrac{T(3)}{1+\cfrac{P(5)}{1+\cfrac{T(5)}{1+\cdots}}}}} . \tag{30}$$

Then, after some algebra, Eq. (29) may be rewritten

$$s_1 = \frac{\omega_1\lambda\cos\varphi}{2I}\,\frac{\phi}{1+\phi+\phi^*} , \tag{31}$$

where

$$I = \tfrac{1}{4}\omega_1^2 \tag{32}$$

and

$$\phi = \cfrac{P(1)}{1+\cfrac{T(1)}{1+\cfrac{P(3)}{1+\cfrac{T(3)}{1+\cdots}}}} . \tag{33}$$

The continued fraction ϕ is simply related with the continued fraction expansion Σ used by Stenholm, namely,

$$\Sigma = (\gamma_1^2/I)\mathrm{Re}\phi . \tag{34}$$

From (31) and (34), Eq. (22) of Stenholm's paper follows immediately. A similar calculation shows that the coefficient s_0 as evaluated from (28) and (25) is identical with the expression (20) given in

the paper by Stenholm and Aminoff.[4]

When both longitudinal and transverse pumpings are present, the odd and even coefficients s_n may be evaluated from (28). Owing to the absence of any interference effect between these two sets of coefficients, the values of s_0 and s_1 which enter the signal expression (22) are mutually independent. Therefore, a misalignment of the pump beam from the directions of the z axis or the x axis may be treated with a simple superposition of the two cases discussed above.

The situation changes appreciably when a misalignment of the rf field is introduced. In this case, the matrices Z_+ and Z_- are not diagonal, since the interference terms $Q(n)$ and $S(n)$ are now different from zero. On the other hand, the coupling terms $P(n)$, $R(n)$, and $T(n)$ are little affected by the rf field misalignment when $\gamma_1 \simeq \gamma_2$ (if $\gamma_1 = \gamma_2$, these terms are completely independent of θ). Therefore, the off-diagonal terms $Q(n)$ and $S(n)$ bring any misalignment effect into the shapes of the resonance curves. As an example, let us consider the solution for the coefficient s_0 at the lowest order in ω_1. This is given by

$$s_0 = \frac{X_0 - [S(0)X_1 + \text{c.c.}]}{1 + R(0) - [S(0)Q(1) + \text{c.c.}]} \,. \tag{35}$$

If the pump beam is perpendicular to the static field, and the rf field is not directed along the x axis ($\theta \neq 0, \pi$), the source terms X_0 and X_{+1}, together with the off-diagonal elements $S(0)$ and $Q(1)$, are different from zero. Furthermore, both X_1 and $Q(1)$ are resonant at $\omega \sim \omega_0$. Therefore, a one-photon transition appears in s_0, giving raise to a resonance at $\omega = \omega_0$. This resonance appears just when θ is different from zero, i.e., it is produced by the misalignment of the rf field. When θ approaches $\frac{1}{2}\pi$, this resonance becomes the parametric resonance, as found by Aleksandrov *et al.*[12] and Favre and Geneux.[1] At high values of the rf field intensity, these resonances are broadened by the rf field power, and one cannot find simple expressions like (35) for the Fourier coefficients: in this case, the matrix continued fraction expansion must be evaluated until convergence is achieved. A few examples of these misalignment resonances will be shown in Sec. IV.

IV. DISCUSSION ON SOME SPECIAL CASES

The solution presented in Sec. III allows one to compute numerically the resonance line shape in any experiment with arbitrary orientations of the rf field and the pumping light beam. Before discussing some cases of interest, we give some details about the numerical evaluation of the matrix continued fraction expansion.

A. Numerical computation

In order to evaluate s_0 and s_1, i.e., the Fourier coefficients which enter the expression (22) for the monitored signal, we need to compute the matrix Z_+; then, using Eq. (13) and its complex conjugate, we express $s_{\pm 3}, s_{\pm 4}$ in terms of $s_{\pm 1}, s_{\pm 2}$, substitute them into system (12) and solve it. This latter step does not need any elucidation, being a standard calculation. The matrix Z_+ has been computed with N and $N+1$ stages. If the moduli of the matrix elements of Z_+ do not change more than 10^{-5} when passing from N to $N+1$ stages, then the matrix continued fraction is truncated, and its value is assumed to coincide with the $(N+1)$th order calculation. Otherwise, a further step is included in the calculation, and comparison is made between the $(N+1)$th and the $(N+2)$th order calculations. The number of required stages to achieve convergence increases when increasing the rf field intensity, or when the static magnetic field is close to a resonance. In our calculations, 10–15 stages are required when the rf field intensity ω_1 was 2–3 times ω, the oscillating field frequency. For a comparison, let us note that the number of stages required in our calculations is one-half the number of stages used in evaluating the Stenholm's continued fraction, since our expansion is a contracted (i.e., more rapidly convergent) form.

B. Static magnetization line shape

In most experiments, where the rf field is linearly polarized, the axis of polarization is chosen to be parallel or perpendicular to the static magnetic field. In the former case, usually referred to as parametric resonance, a transverse magnetization is created whenever $\omega_0 = n\omega$ (n integer, odd or even) if the pump beam is propagating transversally to the static magnetic field. The parametric resonances are neither broadened nor shifted by the rf field. In the other case, i.e., when the axis of rf field polarization is perpendicular to the static field, longitudinal and transverse resonances occur. Let us briefly review their properties. In a longitudinal-resonance experiment, the pumping light beam is directed along the static field, and creates a static magnetization in that direction. In turn, the rf field at resonance tends to equalize the level populations, thus destroying the static magnetization. Therefore, dips in the line shape of the longitudinal magnetization are observed at $\omega = n\omega_0$ (n odd). These dips become broader and shift towards zero static field when increasing the rf field intensity. On the other, in a transverse resonance experiment, a static magnetization is created

by a light beam propagating orthogonally to the static field direction. In this case, peaked resonances in the transverse magnetization occur when $\omega = n\omega_0$ (n even), but their linewidths are little affected by rf field power. The transverse resonances, as the longitudinal ones, are shifted when the rf field is increased. It has been shown in Sec. III that for $\theta = 0°$, the longitudinal and transverse pumpings act independently upon the spin system in inducing longitudinal and transverse static magnetization, respectively. Therefore, if the light beam produces both types of pumpings, the longitudinal and transverse resonances appear independently in the static magnetization parallel or orthogonal to the static field.

If a misalignment of the rf field from $\theta = 0°$ direction is introduced, the situation changes appreciably. In this case, the off-diagonal elements of the matrix Z_+ [Eq. (21)] couple the two phenomena and new resonances appear, as discussed previously. Moreover, the source terms of system (12) are changed: the X_0 and X_1 terms are proportional to the components perpendicular to the static field and to the rf field, respectively. As an example of the phenomena occurring, the static magnetization along the pump beam direction is represented in Figs. 2 and 3 as a function of the static field. The pumping light beam is directed along the x axis, i.e., transversally to the static field, and the rf field orientation is changed from $\theta = 0°$ to $\theta = 90°$. In these figures the lineshapes for one- and two-quantum resonances, respectively, are reported for a rf field intensity $\omega_1/\omega = 0.32$. At $\theta = 0°$, only a two-quantum transverse resonance can be observed, with a very small broadening over the natural linewidth. For

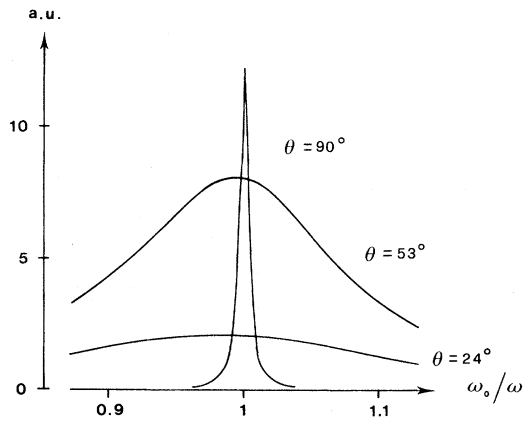

FIG. 2. Transverse static magnetization for a transverse pumping, radio-frequency field amplitude $\omega_1 = 0.32\omega$ and different misalignment angles as function of the static field near the one-quantum resonance value.

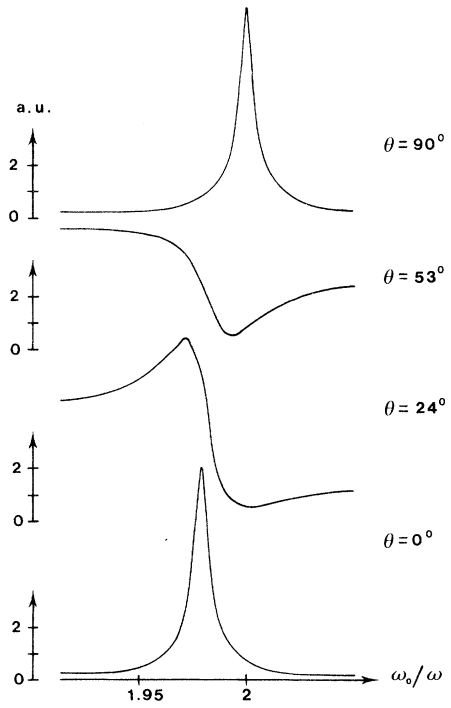

FIG. 3. Transverse static magnetization near the two-quantum resonance value for the same parameters as in Fig. 2. The arbitrary unit of the y axis is 1000 times smaller than in Fig. 2.

$\theta = 90°$, parametric resonances appear for both one- and two-quantum transitions with the natural linewidth. For an intermediate rf field orientation resonances appear with a comparable intensity. Their line shape is a combination of absorption and dispersion part. We have also found that the line shape at strong rf power is mainly determined by the dispersion component. The resonance lines suffer rf power broadening and shift as a function of the rf field component orthogonal to the static field. Resonances for a transverse pumping and rf field arbitrarily oriented in the space have been observed by Aleksandrov *et al.*,[13] but not enough data have been reported to make a comparison with the present theoretical results.

For a fixed value of θ, but different from zero, the off-diagonal terms of the Z_+ matrix have their strongest influence when the light beam is directed along the rf field, if $\gamma_1 = \gamma_2$. In this case, the source terms in the right-hand side of Eqs. (12b) and (12d) vanish. Furthermore, the monitored signal of expression (22) depends upon the s_0 component only. When $\theta = 45°$ and the pumping beam is directed along the rf field, we have found dips in the line shape for all the resonances, with a large asymmetric component at strong rf field

power. This is not surprising, since all the phenomena, for arbitrary orientation of the pumping beam, are masked by the presence of strong longitudinal resonances. In fact, Stenholm has shown that, for a pure transverse rf field, the longitudinal resonances exceed the transverse resonances by a factor ω_1^2/γ_2^2. In our analysis the resonance phenomena shown in Fig. 3 are of the same strength as the transverse resonances. Therefore they are completely masked by the longitudinal ones, when the pumping beam deviates appreciably from the x-axis direction. Thus, if the longitudinal and transverse pumpings have a comparable intensity, the dips created in the line shape by the longitudinal resonances dominate over the resonance signals due to the transverse pumping.

C. Resonance shift

Large attention, from the theoretical and experimental points of view, has been devoted to the shifts of longitudinal and transverse resonances as a function of the rf field intensity (see Ref. 14 and references therein). For longitudinal pumping and rf field orthogonal to the static one, the well-known Bloch-Siegert shift is obtained: the static field at which resonance occurs (at a given frequency of the oscillating field) shifts towards the zero value when increasing the rf power. Measurements of the shift for the one- and three-quantum transitions have been performed by Arimondo and Moruzzi,[15] over a wide range of rf field intensities. The experimental results were compared with the continued fraction solution of Stenholm.[2]

In Fig. 4 the dashed line represents the result of Stenholm's theory: the experimental points are also reported. The rf amplitude ω_1 has been considered up to the value when the one-quantum transition disappears.[3] This value is the smallest root of the equation $J_0(\omega_1/\omega) = 0$, where J_0 is the zeroth-order Bessel function.

The influence of the rf field misalignment on the Bloch-Siegert shift has been investigated by Pegg[6] in the case of small rf field intensities $\gamma_G H_1 \ll \omega$. Through the continued fraction solution the shift may be derived for any value of the rf field: if the angle between rf field and x-axis directions differs from zero by a few degrees, the deviations from the Stenholm's curve cannot be reported on the scale of Fig. 4. Also the competition of longitudinal and transverse resonances when the light beam is arbitrarily directed, but with the rf field orthogonal to the static one, does not produce any appreciable change of the Stenholm result: except for a very large misalignment of the light beam,

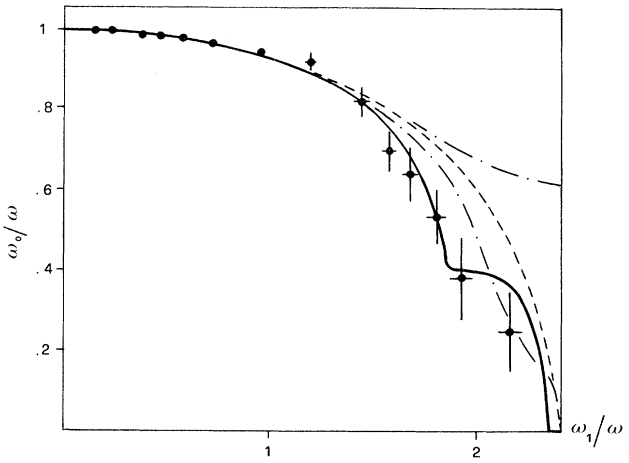

FIG. 4. Bloch-Siegert shift of the one-quantum resonance as a function of the radio-frequency field intensity. Shift without misalignment in the dashed line; $\theta = 2°$ and $\varphi = 11°$ or $-11°$ in the upper or lower chain line, respectively. Shift in the presence of a static stray field in the continuous line.

the transverse resonances are not intense, and their effect on the line shape is negligible.

When both misalignments of rf field and pump beam are present, the deviation from the Bloch-Siegert shift as predicted by Stenholm's theory becomes large, even if introducing only one type of misalignment it was negligible. The chain lines in Fig. 4 represent the behavior for a rf field making an angle $\theta = 2°$ with the x axis, and for the pumping beam making angles $\varphi = +11°$ or $-11°$ with the static field. Very different results are obtained in the two cases, with an increase in the shift if θ and φ have the same sign, or a decrease if the signs are opposite. In the strong rf field region ($\gamma_G H_1 \gg 2.4\omega$), where the theoretical curves have not been reported because of the presence of the zero-field transverse resonance, the occuring phenomena are completely different from the Stenholm's case.

In the experiment of Arimondo and Moruzzi,[15] at low rf power a dip was observed around zero static field, related with the presence of a small static stray field perpendicular to the static one which was swept over the resonance values. The phenomenon has been described as a magnetic resonance transition at zero frequency.[7] Moreover, a check of the rf field misalignment was carried out by observing the intensity of the two-quantum transtion dip. The measurements were performed when that dip was not present in the line shape, indicating that the rf field was well perpendicular to the static field.

It is possible to reproduce theoretically the zero-

frequency signal and the absence of the two-quantum dip in the line shape, by supposing that the static field experienced by the spin system is made up of two parts: the applied static field, in the z-axis direction, and a stray constant field along the x axis. The absence of the two-quantum resonance indicates therefore that the rf field is perpendicular to the direction of the total static field, when the value of the latter one is close to the two-quantum resonance.

The continuous line in Fig. 4 represents the resulting shift for a stray field $\gamma_G H_{\text{stray}} = 0.1\omega$, and for $\theta = 4.5°$ (misalignment of the rf field); $\varphi = 11°$ (angle between the pumping light and the z axis). The double bend shape observed in the theoretical curve at strong rf fields is related to the overlap of the zero-field signal and the zero-field transverse resonance with the one-quantum transition. If one chooses these misalignment parameters, the agreement with the experimental data are impressive, far more as some unpublished details of the line shape observed in the experiment by Arimondo and Moruzzi[15] may be explained. As confirmed by the theory, at very strong rf field the dip observed at zero static field is transformed into a transverse resonance peak. The amplitude of the stray field introduced in the theoretical analysis determines the width of the zero-frequency signal and turns out to be larger than that observed in the experiment. But, if one considers that only two-dimensional misalignments have been introduced in the theoretical analysis, the obtained fit must be considered as completely satisfactory.

V. CONCLUSIONS

The resonance phenomena occurring in a Zeeman-split spin-$\frac{1}{2}$ system interacting with a strong rf field have been investigated for the case in which the static magnetic field, the rf field, and the pumping beams directions are arbitrarily oriented in a plane. The Fourier components of the density matrix are determined by the solution to an infinite set of coupled linear inhomogeneous equations. By limiting attention to the lowest-order terms, a finite set of equations results in which the inhomogeneous terms include contributions from the longitudinal and transverse pumping action. A matrix continued-fraction solution is found which takes into account the rf misalignment.

The solution may be simply extended to the case of a light beam directed out of the plane defined by the static and rf fields. With such an extension the inhomogeneous terms in the equation for the Fourier components of the density matrix would include contributions from the pumping beam action along all three axes.

Numerical calculations for the static magnetization line shape have been given for a few cases investigated experimentally. The influence of the light beam and rf field misalignments on the resonance intensities and shifts has been worked out.

ACKNOWLEDGMENT

The authors wish to acknowledge valuable comments of Dr. Takeshi Oka, and to thank him for the careful reading of the manuscript.

---

*Present address: Herzberg Institute of Astrophysics, National Research Council, Ottawa, Canada K1A OR6.

[1]C. J. Favre and E. Geneux, Phys. Lett. 8, 190 (1964).
[2]S. Stenholm, J. Phys. B 5, 878 (1972).
[3]S. Stenholm, J. Phys. B 5, 890 (1972).
[4]S. Stenholm and C. G. Aminoff, J. Phys. B 6, 2390 (1973).
[5]N. Tsukada and T. Ogawa, J. Phys. B 6, 1643 (1973).
[6]D. T. Pegg, J. Phys. B 6, 241 (1973).
[7]G. W. Series, in *Quantum Optics*, edited by S. M. Kay and A. Maitland (Academic, London, 1970), pp. 395–482.
[8]N. Tsukada and T. Ogawa, Phys. Lett. 45A, 159 (1973).
[9]N. Tsukada and T. Ogawa, J. Phys. Soc. Jpn. 36, 815 (1974); N. Tsukada, T. Koyama, and T. Ogawa, J. Phys. B 7, 799 (1974).
[10]T. Yabuzaki, S. Nagayama, Y. Murakami, and T. Ogawa, Phys. Rev. A 10, 1955 (1974); T. Yabuzaki, Y. Murakami, and T. Ogawa, J. Phys. B 9, 9 (1976).
[11]A. Bambini, Phys. Rev. A 14, 1479 (1976).
[12]E. B. Aleksandrov, O. V. Konstantinov, V. I. Perel', and V. A. Khodovoi, Zh. Eksp. Teor. Fiz. 45, 503 (1963) [Sov. Phys.-JETP 18, 346 (1964)].
[13]E. B. Aleksandrov, O. V. Konstantinov, and V. I. Perel', Zh. Eksp. Teor. Fiz. 49, 97 (1965) [Sov. Phys.-JETP 22, 70 (1966)].
[14]S. Haroche, Ann. Phys. (Paris) 6, 189 (1971); and 6, 327 (1971). A fully quantum-mechanical approach to the Bloch-Siegert shift in strong rf field may be found in S. Yeh and P. Stehle, Phys. Rev. A 15, 213 (1977).
[15]E. Arimondo and G. Moruzzi, J. Phys. B 6, 2382 (1973).